Hydrogen−Deuterium Exchange of Streptavidin and Its Complex with Biotin Studied by 2D-Attenuated Total Reflection Fourier Transform Infrared Spectroscopy

3 AUTHORS, INCLUDING:

Stefan Meskers
Technische Universiteit Eindhoven
199 PUBLICATIONS **6,775** CITATIONS

SEE PROFILE

Jean-Marie Ruysschaert
Université Libre de Bruxelles
472 PUBLICATIONS **13,896** CITATIONS

SEE PROFILE

J. Am. Chem. Soc. **1999**, *121*, 5115−5122

5115

Hydrogen−Deuterium Exchange of Streptavidin and Its Complex with Biotin Studied by 2D-Attenuated Total Reflection Fourier Transform Infrared Spectroscopy

Stefan Meskers,[†] Jean-Marie Ruysschaert,[‡] and Erik Goormaghtigh*,[‡]

Contribution from the Laboratoire de Chimie-Physique des Macromolécules aux Interfaces, CP 206/2, Université Libre de Bruxelles, Campus Plaine, B-1050 Brussels, Belgium, and Laboratory of Macromolecular and Organic Chemistry, Eindhoven University of Technology, P.O. Box 513, NL-5600 MB Eindhoven, The Netherlands

Abstract: Hydrogen−deuterium exchange for streptavidin and its complex with biotin is studied by means of attenuated total reflection (ATR) Fourier transform infrared (FTIR) spectroscopy. To analyze the spectral changes upon deuteration, difference spectra and two-dimensional correlation spectra are calculated. We find that the exchange rate varies with the secondary structure in which the exchanging amide protons are incorporated. The most slowly exchanging protons, with a characteristic time constant on the order of hours, are part of the β-sheet secondary structure. The separation in time of exchange of the β-sheet from other structural elements allows the amide II and II' frequencies of the β-sheet (1530 and 1445 cm^{-1}) to be identified. A second component which exchanges more rapidly than the β-sheet is characterized by its amide I frequencies 1680, 1640, and 1465 cm^{-1}. This component is attributed to the exchange of amide groups in secondary structures other than the central β-barrel. Binding of the ligand results in a slower exchange rate of the rapid component. These changes are interpreted in terms of structural differences observed by previous X-ray studies of one loop in the protein involved in the binding of the ligand. The presence of the ligand is found to inhibit the exchange of ∼10 amide protons during the time of the experiment (10 h). The protected amide groups are most likely part of the β-sheet structure, and their retarded exchange is tentatively interpreted in terms of a reduced flexibility of the tetrameric protein upon binding of the ligand.

Introduction

While our knowledge of protein secondary and tertiary folding steadily increases, information about how enzymes change their conformation and their dynamic properties during their catalytic activity remains scarce.

The analysis of distinct IR spectral regions can provide us with information on both protein structure and its dynamics. Because the different secondary structures absorb in different regions of the amide I (1700−1600 cm^{-1}), this band has been used for a long time to extract information on the secondary structure content of proteins[1,2] (for a review, see Goormaghtigh et al).[3] Detection of the intensity changes in the amide II (1600−1500 cm^{-1}) or amide II' (1500−1400 cm^{-1}) regions upon exposure of a protein to D$_2$O provides information on the tertiary stability of the protein at a molecular level. These changes have been shown to reflect the exchange of labile amide protons, whose exchange rates are determined by solvent accessibility[4] and by the conformational flexibility of the protein as well as

its embedding within the lipid membrane.[5−7] Combining H/D exchange with FTIR spectroscopy offers a unique opportunity to obtain a detailed description of the conformational changes that accompany ligand binding.

As a first step in this type of analysis, we have chosen streptavidin, a well-characterized protein whose structure is known from X-ray crystallographic studies.[8−10] The protein is a homotetramer (158 residues per monomer). It binds biotin with very high affinity ($K_d = 4 \times 10^{-14}$ M[11]).

Attenuated total reflection (ATR) FTIR spectroscopy is a sensitive and convenient method to record IR spectra of proteins, especially membrane proteins. Although one works with protein films when the ATR-IR approach is applied, it has been shown that differences in tertiary stability of a protein are characterized both in films and in aqueous solution by similar differences in amide proton exchange rates.[12] It was also demonstrated that

---

† Université Libre de Bruxelles.

‡ Eindhoven University of Technology.

* To whom correspondence should be addressed. Telephone: (32) 2 6505386. Fax: (32) 2 6505113. E-mail: egoor@ulb.ac.be.

(1) Susi, H.; Timasheff, S. N.; Stevens, L. *J. Biol. Chem.* **1967**, *242*, 5460.

(2) Timasheff, S. N.; Susi, H.; Stevens, L. *J. Biol. Chem.* **1967**, *242*, 5467.

(3) Goormaghtigh, E.; Cabiaux, V.; Ruysschaert, J.-M. *Subcell. Biochem.* **1994**, *23*, 405.

(4) Goormaghtigh, E.; Vigneron, L.; Scarborough, G.; Ruysschaert, J.-M. *J. Biol. Chem.* **1994**, *269*, 27409.

(5) Vigneron, L.; Ruysschaert, J.-M.; Goormaghtigh, E. *J. Biol. Chem.* **1995**, *270*, 17685.

(6) Raussens, V.; Narayanaswami, V.; Goormaghtigh, E.; Ryan, R. O.; Ruysschaert, J. M. *J. Biol. Chem.* **1996**, *271*, 23089.

(7) Raussens, V.; Ruysschaert, J.-M.; Goormaghtigh, E. *J. Biol. Chem.* **1997**, *276*, 262.

(8) Weber, P. C.; Ohlendorf, D. H.; Wendoloski, J. J.; Salemme, F. R. *Science* **1989**, *243*, 85.

(9) Hendrickson, W. A.; Paehler, A.; Smith, L. J.; Satow, Y.; Merrit, E. A.; Phizakerley, R. P. *Proc. Natl. Acad. Sci. U.S.A.* **1989**, *86*, 2190.

(10) Freitag, S.; Le Trong, I.; Klumb, L.; Stayton, P. S.; Stenkamp, R. E. *Prot. Sci.* **1996**, *6*, 1157.

(11) Green, N. M. *Methods Enzymol.* **1990**, *184*, 51.

(12) de Jongh, H. H. J.; Goormaghtigh, E.; Ruysschaert, J.-M. *Biochemistry* **1995**, *34*, 172.

the apparent pH in protein films spread from buffered aqueous solutions can be retained[12] and that a similar pH dependency of the exchange rates which is OH^{−} catalyzed has been found for a protein in a film and in aqueous solution.[13]

The amide I, primarily arising from C=O stretching (70−85% of the potential energy) together with an out-of-phase CN stretching, a CCN deformation, and a small NH in-plane bending contribution,[14] generally shifts by 5−10 cm^{−1} to lower wavenumber upon exposure of a protein to an D_2O environment as recently reviewed.[3,15] While global exchange rate of a protein is conveniently monitored by amide II intensity decay, information specific to different secondary structures is available in amide I. Recently, detection of the shifts in different regions of amide I was shown to give access to information on the stability of the individual secondary structure types of a protein.[16,17]

Furthermore, because H/D exchange does not happen at the same rate for all the secondary structures, the kinetic analysis of the frequency shifts observed in the course of the exchange should help resolve the complex substructure of the amide bands. In this paper, we investigate the spectral region from 1400 to 1700 cm^{−1}. The amide I and II bands fall in this region as well as the amide I′ and II′ of the deuterated protein. In general, these bands consist of several subbands arising from the different secondary structure domains in the protein. We show that differences in the exchange kinetics of these subdomains can be used to establish which subbands in the amide bands I, I′, II, and II′ originate from the same secondary structure type.

In this study, we also investigate the effect of ligand binding on the hydrogen deuterium exchange to see whether ligand binding influences the dynamic properties of the protein and furthermore, to see whether it is possible to distinguish subtle differences within secondary structure types, and to assign their frequencies in the 1400−1700 cm^{−1} spectral range.

Experimental Section

Materials. Streptavidin, biotin, and dimyristoylphosphatidylcholine (DMPC) were obtained from Sigma Chemicals used without further purification.

Sample Preparation. Protein and biotin solutions were prepared in 2 mM Hepes/Tris buffer solution (pH 7.2). The protein and biotin concentration were determined by weight. Biotin−protein mixtures were incubated for at least 1 h at room temperature before use, and a small excess of biotin was used (∼10%). Final pHs of protein and protein−biotin solution were checked and found to be the same within the accuracy of the pH meter (∼0.05 pH unit).

Methods. Spectra were recorded with a Bruker IF55 Fourier transform infrared spectrophotometer equipped with a mercury cadmium telluride detector with a resolution of 2 cm^{−1}. A volume of the sample solution corresponding to 70 μg of protein was spread on a germanium ATR plate and dried by passing a stream of nitrogen over the plate. Before the sample solution was spread, the germanium surface was rendered hydrophilic by treatment with basic detergent, washing with methanol and chloroform, and finally cleaning in a plasma cleaner (PDC-23G, Harrick, NY). Hydrogen deuterium exchange was effected by passing a stream of D_2O-saturated nitrogen gas over the protein film. Spectra for protein samples with and without biotin were collected using a sample shuttle. The beginning of the second sample started only 20 min after the first one, ensuring similar experimental conditions

for streptavidin and streptavidin/biotin. Details about the use of the shuttle can be found in Vigneron et al.[5]

Data Manipulation. The small contribution of water vapor to the final (background subtracted) spectra was eliminated by subtracting a separately measured spectrum of water vapor. After this subtraction, the spectra were smoothed using Gaussian apodization and this lowered the resolution to 4 cm^{−1}. When indicated (Figure 5), spectra were Fourier self-deconvolved with a Lorentzian line-shape (full width at half-height, fwhh = 20 cm^{−1}) and apodized by a Gaussian line-shape (fwhh = 10 cm^{−1}).

Correlation Spectroscopy. 2D correlation spectra were calculated following the method by Noda[18] as recently described by Nabet and Pézolet.[19]

From the measured intensity y at time $t + \tau$, a reference intensity measured at time t is subtracted according to eq 1. The Fourier transform in the time domain of the N collected spectra is calculated according to eq 2.

$$\tilde{y}(\nu,\tau) = y(\nu,t+\tau) - y(\nu,t) \tag{1}$$

$$\tilde{Y}(\nu,g) = \frac{1}{N}\sum_{\tau=0}^{N-1}\tilde{y}(\nu,\tau)\exp\left(-\frac{2i\pi\tau g}{N}\right) \tag{2}$$

Synchronous ($\Phi(\nu_1,\nu_2)$) and asynchronous ($\Psi(\nu_1,\nu_2)$) are then calculated according to eqs 3 and 4.

$$\Phi(\nu_1,\nu_2) = \frac{1}{\pi N}\sum_{g=0}^{N}Re(\tilde{Y}(\nu_1,g))\,Re(\tilde{Y}(\nu_2,g)) + Im(\tilde{Y}(\nu_1,g))\,Im(\tilde{Y}(\nu_2,g)) \tag{3}$$

$$\Psi(\nu_1,\nu_2) = \frac{1}{\pi N}\sum_{g=0}^{N}Im(\tilde{Y}(\nu_1,g))\,Re(\tilde{Y}(\nu_2,g)) + Re(\tilde{Y}(\nu_1,g))\,Im(\tilde{Y}(\nu_2,g)) \tag{4}$$

The 2D correlation spectra were interpreted using the rules described by Noda[20] and more recently by Ekgasit et al.[21]

Difference Spectroscopy. To calculate differences between two spectra of protein with different degree of deuteration accurately, use was made of an internal reference. The C=O stretch band of the lipid DMPC located at 1735 cm^{−1} was used. The spectrum to be subtracted was scaled in such a way that the resulting difference spectrum gave the best fit to a straight line in the region from 1780 to 1720 cm^{−1}. A computer algorithm (part of the software package SAFAIR obtained from Dr. K. Oberg) implemented in the commercially available software package Spectracalc (Galactic Industries) was used to calculate the difference spectra automatically. Upon deuterium substitution, the frequencies of the bands are known to be lowered by approximately 5−15 cm^{−1}. Accordingly the difference spectrum between the D and H form is expected to consist of sigmoidal features at these frequencies. However, due to overlap of the bands of the H and D form, the extrema in the H−D difference spectrum do not correspond to the frequencies of the original bands. To solve this problem and to obtain usable information, we suggest here a solution that relates the band shift upon exchange, $\Delta\nu$, to the frequency separation, D, that can be measured on the difference spectra between the maximum and minimum of the S-shaped features. The bands were supposed to be Lorentzian in shape in order to obtain an analytical solution to the problem. The difference spectrum diff(ν) obtained by subtracting a band of fwhh and shifted by $\Delta\nu$ cm[−1] is described by

$$\text{diff}(\nu) = \frac{\text{fwhh}^2}{\text{fwhh}^2 + 4(\nu - \Delta\nu)^2} - \frac{\text{fwhh}^2}{\text{fwhh}^2 + 4\nu^2} \tag{5}$$

To determine the frequency of the extrema in the difference spectrum, the derivative of this expression was set equal to 0 and solved for ν,

(13) Goormaghtigh, E.; de Jongh, H. H. J.; Ruysschaert, J.-M. *Appl. Spectrosc.* **1996**, *50*, 1519.

(14) Krimm, S.; Bandekar, J. *Adv. Prot. Chem.* **1986**, *38*, 181.

(15) Goormaghtigh, E.; Cabiaux, V.; Ruysschaert, J.-M. *Subcell. Biochem.* **1994**, *23*, 363.

(16) de Jongh, H. H. J.; Goormaghtigh, E.; Ruysschaert, J.-M. *Biochemistry* **1997**, *36*, 13593.

(17) de Jongh, H. H. J.; Goormaghtigh, E.; Ruysschaert, J.-M. *Biochemistry* **1997**, *36*, 13603.

(18) Noda, I. *Appl. Spectrosc.* **1990**, *44*, 551.

(19) Nabet, A.; Pézolet, M. *Appl. Spectrosc.* **1997**, *51*, 466.

(20) Noda, I.; Dowrey, A. E.; Marcott, C., *Appl. Spectrosc.* **1993**, *47*, 1317.

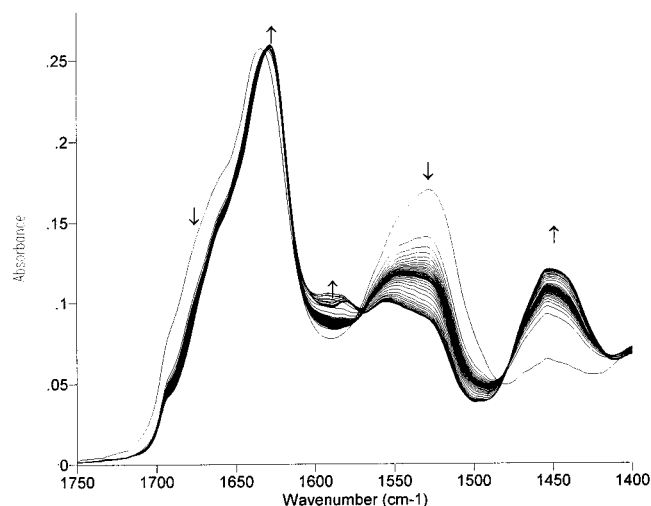(21) Ekgasit, S.; Ishida, H. *Appl. Spectrosc.* **1995**, *49*, 1243.

Figure 1. ATR-FTIR spectra of 70 μg of (apo)streptavidin on a germanium crystal recorded during the H/D exchange. The protein film was cast from 7 μL of protein solution in 2 mM Hepes/Tris buffer (pH 7.2) Time points at which spectra were taken vary from 0 to 636 min after the start of the D$_2$O-saturated N$_2$ flow over the protein film on the germanium crystal. Spectra were recorded every 30 s from 0 to 10 min, then after 13, 17, 33, 49, 96, 156, 216, 276, 336, 396, 456, 516, 576, and 636 min after the beginning of the kinetics. The arrows indicate the direction of the intensity change during the exchange.

yielding two real solutions:

$$\nu_{\text{max,min}} = \frac{1}{2}\Delta\nu \pm \frac{\sqrt{3}}{6}\sqrt{\Delta\nu^2 - \text{fwhh}^2 + 2\sqrt{\text{fwhh}^4 + \text{fwhh}^2\Delta\nu^2 + \Delta\nu^4}} \quad (6)$$

The frequency separation D between the two maxima in the difference spectrum is obtained as the difference between ν_{max} and ν_{min} given in eq 6. After simplification, it is described by

$$D = \frac{\sqrt{3}}{3}\sqrt{\Delta\nu^2 - \text{fwhh}^2 + 2\sqrt{\text{fwhh}^4 + \text{fwhh}^2\Delta\nu^2 + \Delta\nu^4}} \quad (7)$$

which can be solved for $\Delta\nu$:

$$\Delta\nu = \sqrt{-\text{fwhh}^2 - D^2 + 2D\sqrt{\text{fwhh}^2 + D^2}} \quad (8)$$

Expression 8 describes how the band shift upon deuteration, $\Delta\nu$, is related to the frequency separation of the extrema, D, in the difference spectrum. It appears that this expression also depends on the fwhh of the band that experience the shift.

Results and Discussion

H/D Exchange. In Figure 1 we show the result of a typical H/D exchange experiment. Shown are the changes in intensities of the absorption bands of streptavidin in the 1750−1400 cm^{-1} spectral region during the course of the deuteration. The spectra were recorded at defined time points in the intervals 0−10 h after the start of the flow of D$_2$O-saturated nitrogen gas over the protein film on the ATR crystal.

As can be seen on Figure 1, there is a gradual increase of the amide II′ band near 1450 cm^{-1} accompanied by a decrease of the amide II band near 1540 cm^{-1}. An isobestic point occurs near 1480 cm^{-1}. In the amide I band (between 1700 and 1600 cm^{-1}), a decrease of the absorbance at high wavenumbers and an increase at low wavenumbers occurs. It is well-known that the subbands under the amide I envelope shift a few wavenumbers to lower frequency upon deuteration. Due to the overlap of these bands, deuteration results in a net decrease of the
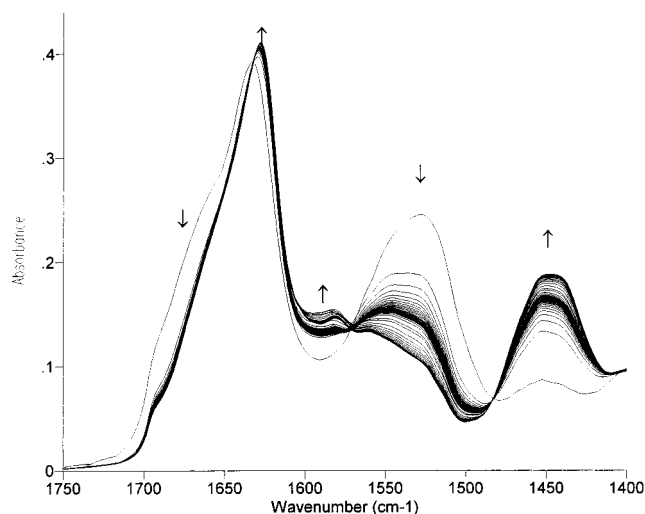

Figure 2. ATR-FTIR spectra of 70 μg of streptavidin−biotin complex during the H/D exchange. For details see legend of Figure 1.
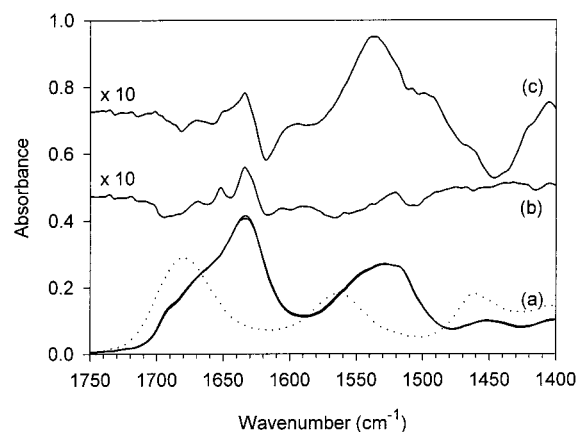

Figure 3. ATR-FTIR spectra for the undeuterated forms of streptavidin and the streptavidin−biotin complex (a, solid lines). The difference spectrum obtained by subtraction of the spectrum of streptavidin alone from the spectrum of the streptavidin−biotin complex is computed before (b) and after 4 h of exposure to D$_2$O vapor (c). An ATR-FTIR spectrum for biotin is shown as dashed line.

intensity at the high-frequency side of the amide I band and increase at the low-frequency side.

For comparison we show in Figure 2 the series of IR spectra recorded during the deuteration of the streptavidin−biotin complex. The spectra before deuteration are very similar; indicating that the ligand binding does not affect significantly the secondary structure of the protein. This is further illustrated in Figure 3, where the spectra for the protein alone and for the streptavidin−biotin complex are overlaid (see a). Shown in the upper part of the graph are the differences between spectra of the bound and free form of the protein before deuteration (b) and after 10 h of exposure to D$_2$O (c). Interestingly, biotin (Figure 3, bottom, dotted line) has a moderately strong absorption band at 1460 cm^{-1} (assigned to CH vibrations), with an intensity approximately half of its strongest absorption band at 1680 cm^{-1} (assigned to the carbonyl of the ureidino moiety (Figure 3, dotted line)). Yet, near 1460 cm^{-1}, the difference spectrum is practically zero. We therefore conclude that the contribution of biotin to the total absorbance is negligible and that the differences in absorbance at other frequencies are mainly due to small changes in protein secondary structure upon ligand binding.

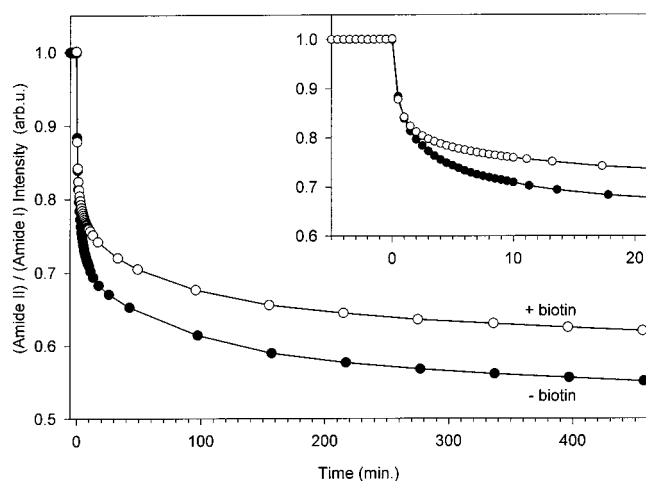The difference between free and ligand bound proteins after

Figure 4. Integrated amide II intensity referenced to the integrated amide I intensity of streptavidin (spectra shown in Figure 1) as a function of time after the start of H/D exchange. The insert shows the early time period of the experiment. Integration limits: amide I, 1700–1600 cm^{-1}; amide II, 1560–1500 cm^{-1}. No further baseline corrections were made for the integration. The time points before 0 have been recorded before starting the D_2O/N_2 flow.

10 h of deuteration (Figure 3, curve c) is significantly larger than before (Figure 3, curve b). For the streptavidin–biotin complex, a higher absorbance in the amide II and a lower absorbance in the amide II′ region is observed after deuteration indicating a lower degree of deuteration when the ligand is bound. To quantify this further we have plotted in Figure 4 the integrated amide II intensity referenced to the amide I integrated intensity as a function of time.[22] The lower degree of deuteration in the presence of biotin is also evident from this graph. As can be seen from Figure 4, the difference in the degree of deuteration arises quite early in time and remains constant after 120 min.

Difference Spectra. To attempt to assign the exchange process to different secondary structure types in the protein, we calculated the differences between consecutive spectra recorded during the experiment. The information on the nature of the exchanging secondary structure should be contained in the position of the peaks in the difference spectra. To calculate these differences accurately we added the lipid dimyristoylphosphatidylcholine (DMPC) as an internal standard to the sample. DMPC has an absorption band at 1735 cm^{-1} but no band in the amide I and II region. The presence of the lipid did not influence the exchange kinetics of the protein to any measurable extent (data not shown).

For the streptavidin and streptavidin–biotin complex, differences between pairs of successive spectra measured at 0,1, 2, 4, 8, 16, 30, 60, and 120 min after the start of the flow of D_2O-saturated nitrogen are shown in Figure 5. We also show the difference between spectra taken between 360 and 600 min after the start of the experiment. The uppermost spectra in the left and right panels of the figures will be discussed later. The original spectrum as well as the Fourier self-deconvolved spectrum are presented on top of the difference spectra. In agreement with the high β-sheet content in the protein (Table 2), two main features appear in the amide I near 1690 and 1630 cm^{-1}, characteristic of the β-sheet structures (for a review, see Goormaghtigh et al.[3]).

As can be seen, the amplitude in the first difference spectrum (1−0 min) is approximately 20 times larger than in the second

spectrum (2−1 min). Apparently a large number of the amide protons exchange very rapidly under the experimental conditions.

First we discuss the difference spectra pertaining to streptavidin without ligand (right panel of Figure 5). Looking at the late difference spectra (between 120 and 60 min or 600 and 360 min) we observe two main S-shaped features. The first one presents a minimum at 1695 cm^{-1} and a maximum at 1685 cm^{-1}, while the second one has a minimum at 1634 cm^{-1} and a maximum at 1620 cm^{-1}. In agreement with the documented slow exchange of β-sheet structures[16,17] we assign these features to the exchange of β-sheet amide protons. This assignment is also in agreement with the known infrared spectrum of β-sheet which presents two bands in the amide I region. A high-frequency component (called B1) is observed between 1695 and 1675 cm^{-1} and a main band (called B2), about 10 times as intense as the former, between 1623 and 1641 cm^{-1} (for a review, see Goormaghtigh et al.[3]). Upon deuterium substitution, the frequencies of these two bands are known to be lowered by approximately 5−10 cm^{-1}. Accordingly the difference spectrum between the D and H form of β-sheet is expected to consist of two sigmoidal features at these frequencies. However, due to overlap of the bands of the H and D form, the extrema in the H−D difference spectrum do not correspond to the frequencies of the original bands. To solve this problem and get usable information, we therefore used the method described in the Experimental Section. For the β-sheet structure, values of 17 cm^{-1} (near 1620 cm^{-1}) and 9 cm^{-1} (near 1690 cm^{-1}) have been reported for the band fwhh.[23,24] Since we are looking at a well-ordered β-sheet component, it seems reasonable to consider a fwhh of 17 cm^{-1} near 1620 cm^{-1}. The frequency separation D between the extrema of the S-shaped features observed in Figure 5 for the β-sheet contribution is about 15 cm^{-1} for the low-frequency band and 7−10 cm^{-1} for the high-frequency band. Using eq 8 we find a shift $\Delta\nu$ of the absorbance band is ca. 13 cm^{-1} for the low-frequency band and 6−9 cm^{-1} for the high-frequency component. It comes that the low-frequency component shifts from 1633 to 1620 cm^{-1} and the high-frequency component from 1694 to 1686 cm^{-1} in complete agreement with the known behavior of β-sheet upon H/D exchange.

Finally, it is of interest to note that the slowly exchanging β-sheet component presents a negative broad band centered around 1530 cm^{-1} and a positive band around 1440 cm^{-1} assigned to the amide II and amide II′ contributions.

As can be seen in Figure 5, the difference spectra change gradually with time, indicating that different secondary structures exchange with different rates. While the above discussion focused on the slowly exchanging β-sheet component only, we note the following changes in the time course of the experiment. First, a negative band at 1680 cm^{-1} is present in the early difference spectra and disappears after 60 min. Second, the main maximum in the amide I difference spectrum shifts with time from 1625 to 1618 cm^{-1}. Third, while little shift is visible in the amide II region, there is a gradual displacement of the maximum near 1460 cm^{-1} toward lower wavenumbers (1440 cm^{-1}). Finally, we note the appearance of bands in the difference spectra near 1580 cm^{-1}, a region normally not associated with amide backbone vibrations. Bands around 1580 cm^{-1} in the difference spectra display both rapid and slow changes and are most likely due to amino acid side chains, probably the guanidino group of Arg and/or the carboxylate group of Asp

(22) de Jongh, H. H. J.; Goormaghtigh, E.; Ruysschaert, J. M. *Anal. Biochem.* **1996**, *242*, 95.

(23) Chirgadze, Y. N.; Shestopalov, B. V.; Venyaminov, S. Y. *Biopolymers* **1973**, *12*, 1337.

(24) Goormaghtigh, E.; Cabiaux, V.; Ruysschaert, J.-M. *Subcell. Biochem.* **1994**, *23*, 329.
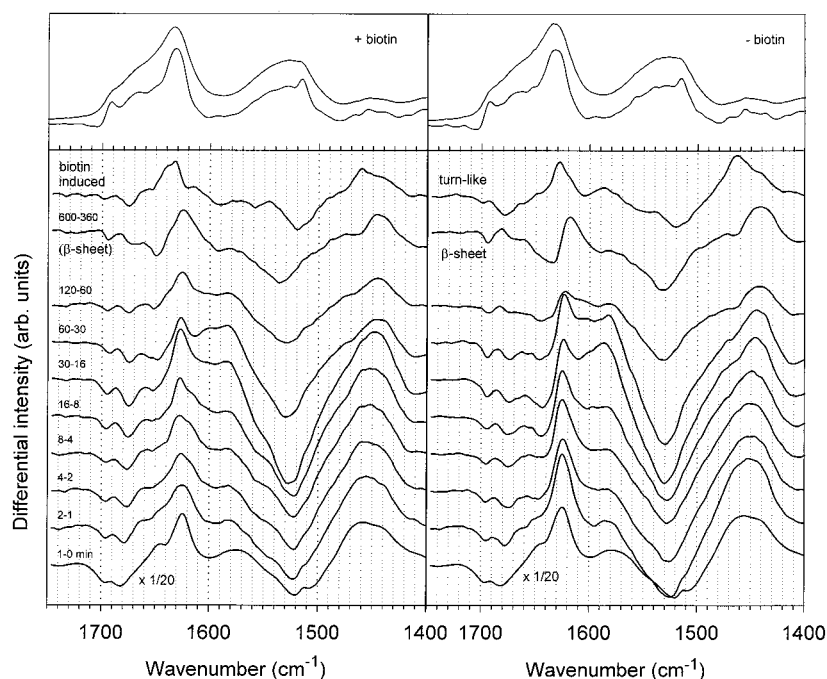
Figure 5. Differences between spectra taken at different time points (indicated on the left side) during the course of deuteration: left column, holostreptavidin; right column, apo-streptavidin. Uppermost spectra in both columns labeled "biotin induced" and "turn-like" result from manipulation of the other spectra shown (see text). A positive amplitude in the difference spectrum implies an increase in intensity during exchange at that frequency. The series of difference spectra for streptavidin−biotin were scaled by the same constant, such that the maximum intensity of the amide I peak before deuteration is the same for both free and ligand-bound forms.

Table 1. Summary of the Major Anticorrelation and Correlation Features[a]

		1407	Slow beta 1445	Fast beta 1465	1475	Tyr 1511	beta 1530	1538	1580	Side-chains 1585	Side-chains 1610	Slow beta 1622	Fast beta 1640	Turns 1658	Turns 1675	Turns 1680-1685	Slow beta 1695
1407			1407						1407			1407					
1445	↗		1445	1445						1445					1445	1445	
1465			1465		1465		1465				1465	1465					1465
					1475												
1511				1512													
1530	↘		1530	1530		1535		1546		1530		1530				1530	
1580	↗			1580												1580	
1585	↗		1580				1585		1585			1585					1585
1610																	
1622	↗		1622	1630	1610		1622			1622		1622				1622	1622
1640	↘											1640		1640			
1658	↘, l									1650							
1675	↘, s		1675							1675		1675				1675	
1680-1685	↗, l			1680			1680					1685			1685		1685
1695	↘			1695						1695		1695				1695	

[a] The first line of the table reports the main frequencies (cm⁻¹) where anticorrelation peak appears. The frequencies which anticorrelate are found below in the column. The two major groups of frequencies discussed in the text are framed with solid or dotted lines. The curved up/down arrows indicate whether the intensity decreases or increases according to the correlation 2D map (Figure 6, right panel). Tentative assignments are reported on top of each column.

and Glu residues.[24-26] Solvent-exposed side chain groups usually exchange very quickly. However, salt bridges between Arg and Asp residues might explain the slow exchange observed.

Because of the overlap of the different components present in the spectra, difference spectroscopy or Fourier self-deconvolution cannot resolve them any further. In a second step, we have used 2D correlation techniques to resolve important components of the spectra.

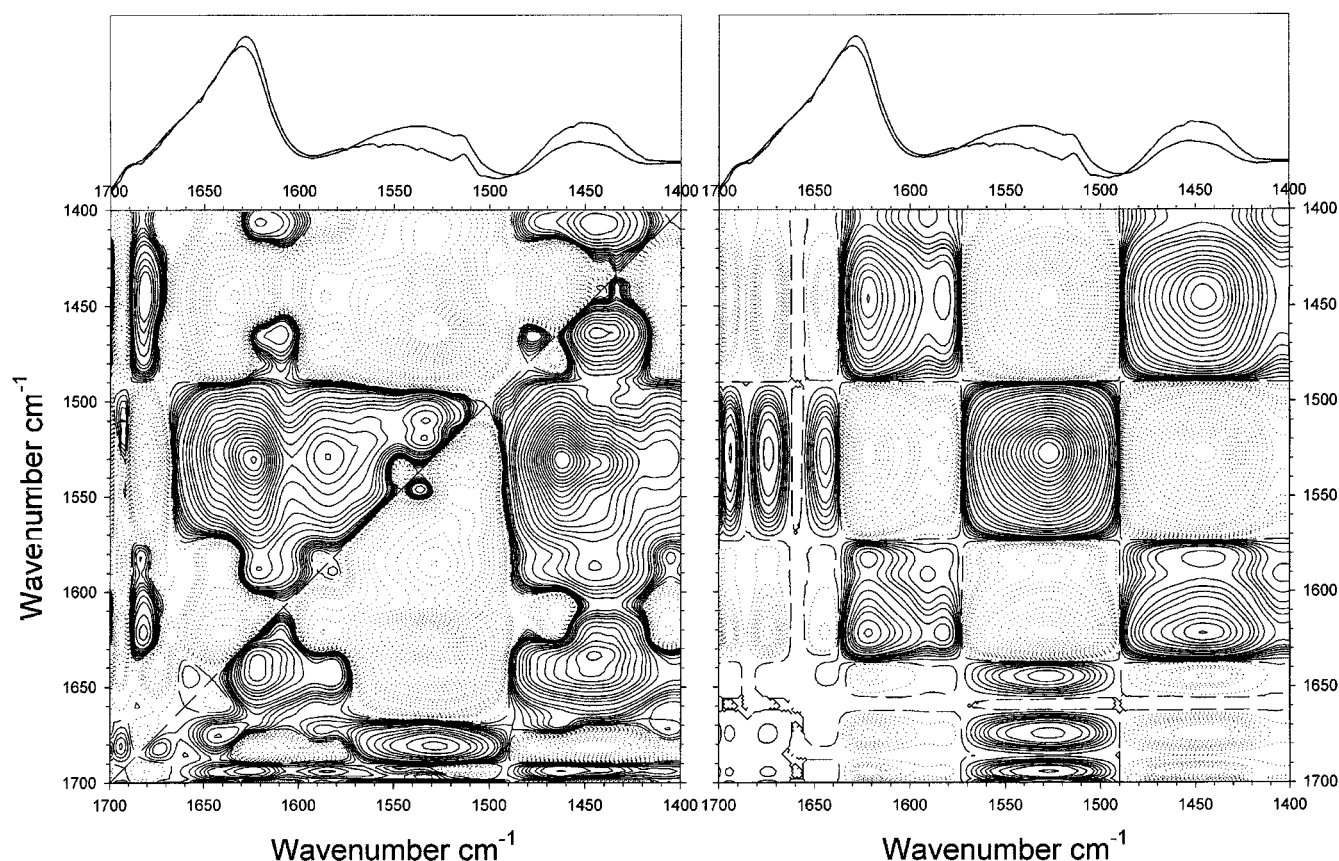**2D Correlation Analysis for Apo-streptavidin.** As a tool

(25) Chirgadze, Y. N.; Feodorov, O. V.; Trushina, N. P. *Biopolymers* **1975**, *14*, 679.
(26) Venyaminov, S. Y.; Kalnin, N. N. *Biopolymers* **1990**, *30*, 1243.

Figure 6. Left panel: asynchronous 2D correlation spectra for H/D exchange of streptavidin. Time window: 1.5−600 min after the start of D$_2$O flow. Solid lines represent positive contours, dotted lines negative ones. The spectra are by definition antisymmetric across the diagonal. Contour lines are drawn at a log interval. Right panel: synchronous correlation map.

Table 2. Number of Amino Acid Residues per Secondary Structure Class in the Crystal Structure of Streptavidin[a]

	β-sheet	irreg.	bend	turn	α-helix	3_{10} helix	total[b]
streptavidin	68	23	16	5	2	8	122 (77%)
streptavidin−biotin	67	24	14	6	4	6	121 (77%)

[a] Numbers were obtained from analysis of the structures with PDB code 1stp and 1slf using the procedure by Kabsch and Sanders (1983). When two chains were present in the structure, the average values were taken. [b] Total number of residues included in the structure model and percentage of the total number of residues in the protein.

to analyze the H/D exchange kinetics further, we have applied two-dimensional correlation analysis[20] to the series of spectra shown in Figure 1, using eqs 1−4 as described in the Experimental Section. As in the first minute of the exchange kinetics, a number of processes take place such hydration and swelling of the protein film which may be superimposed to the exchange process,[16,22] we decided to analyze only changes occurring after 1.5 min (t in eq 1 is set to 1.5 min). In turn, in the subsequent analysis, the fastest exchanging components which include the disordered part of the structure and probably a fraction of the turns, will not be considered. It is important to note here that ca. 25% of the amide protons are already exchanged before we start the analysis. As noted in earlier applications of 2D correlation analysis,[19,27] we found the so-called disrelation or asynchronous correlation spectrum to be more informative. Essentially, the asynchronous correlation spectrum shows the degree of disrelation between the kinetic of the changes in the intensity at two different wavelengths. If the kinetic rate constant for the changes in intensity are different,

a cross-peak appears in the 2D asynchronous correlation plot. The sign of the cross-peak can be either positive or negative, depending on whether the changes at frequency 1 lead or lag behind those at frequency 2. The absence of a cross-peak between two frequencies implies that the changes in intensity occur with nearly the same rate. By definition, the spectrum is antisymmetric across the diagonal.

Figure 6, left panel, reports the anticorrelation 2D map between 1700 and 1400 cm^{-1}. The solid lines represent positive contours while dotted lines show the negative ones. We note that the dotted contours, which are difficult to trace, appear as positive contours across the diagonal of the spectrum and are more clearly visible there. Also shown along the abscissa of the 2D spectra are the ordinary 1D spectra of the proteins before and after 360 min of exposure to the D$_2$O flow.

A first important information comes from the observation of several peaks close to the diagonal. These peaks indicate the presence of nonhomogeneous kinetic behavior at two close frequencies. Major disrelations found within 20 cm^{-1} appear between 1695/1680, 1680/1675, and 1645/1622 cm^{-1} in the amide I region, 1546/1538 cm^{-1} in the amide II region, and 1465/1445 and 1465/1475 cm^{-1} in the amide II′ region. The anticorrelation analysis is therefore able to resolve components of the spectrum close in frequency but characterized by different H/D exchange kinetics. All the cross-peaks mentioned above appear on Figure 6, left panel, and are italicized in Table 1.

To get an overall picture of the information contained in the 2D anticorrelation map, it is useful to observe that the main intensity spots are located at a limited number of well-defined frequencies: 1445, 1465 cm^{-1} in amide II′, 1530, 1585 cm^{-1} in amide II, and 1622, 1680−1685 cm^{-1} in amide I. These

(27) Burie, J.-R. *Appl. Spectrosc.* **1996**, *50*, 861.

frequencies can be separated in two main groups: 1445, 1530, 1622, and 1695 cm^{-1} (dotted frames in Table 1) which systematically anticorrelates with the other group, 1465, 1585, 1658, and 1685 cm^{-1} (solid frames in Table 1). That the members of one of the group do not disrelate one with another can be checked by the absence of cross-peak among them on Figure 6 or in Table 1 with the only exception of 1622 cm^{-1}, which disrelates with 1530 and 1695 cm^{-1}. We suggest here that this anomaly is due to the large intensity change at 1622 cm^{-1}, which enhance very small kinetic differences. So, all the components of one group have roughly similar exchange kinetics which, however, differ markedly from these observed for the other group. It is therefore possible that all the members of each group belong to a same secondary structure and it is certain that all the members of the other group belong to another part of the protein with a different H/D exchange dynamics. In a first approximation the 2D correlation plot may therefore be understood in terms of two major protein secondary structure types exchanging at different rates; the β-sheet structure with absorption bands at 1622, 1530, and 1445 cm^{-1} as already described on the basis of the difference spectra and one or several structures with bands at 1685, 1675, 1658, 1640, 1585, and 1465 cm^{-1}. It is interesting to point out that the present approach helps assignments in the amide II and II′ regions which are usually poorly investigated.

The disrelation spectrum in the amide I region is more difficult to interpret. In the amide I band area, a number of frequencies are characterized by weak anticorrelation cross-peaks. Yet, the 1640/1622 cm^{-1} cross-peak is well-marked and provides an interesting insight into the β-sheet structure IR component in the amide I region. The presence of this cross-peak thus indicates that two distinct structures absorbing in the β-sheet region of amide I. The 1695/1680 and 1680/1675 cm^{-1} cross-peaks are weak, and it is more difficult to assign them to a particular structure. However, they are consistently present in these experiments. We tentatively assign 1695 and 1622 cm^{-1} to β-sheet as already discussed on the basis of difference spectroscopy data (Figure 5) and 1640 cm^{-1} to a second type of β-sheet. It is important to stress here that it does not imply here that the secondary structure is strikingly different in terms of its geometry, the results only indicate a marked difference in the exchange rate. In the amide II′ region, the 1465 cm^{-1} frequency disrelates with the slow β-sheet but not with the fast one. It is therefore likely that the fast β-sheet structure has a component at 1465 cm^{-1} in the amide II′. The other frequencies (1658, 1675, and 1680 cm^{-1}) could be due to the turn contributions. Careful analysis of the 2D correlation map calculated over shorter period of time (from 1.5 to 10 min, from 10 to 50 min, and from 50 to 600 min, data not shown) indicates that 1675 cm^{-1} component appears only in the second part of the kinetic while the 1680 and 1658 cm^{-1} components are present at the beginning of the kinetic in agreement with a faster exchange usually found for turn structures. Other frequencies such as 1610 and 1585 cm^{-1} are most likely associated to the exchange of amino acid side chains.

Though less detailed than the anticorrelation map, the correlation map (Figure 6, right panel) allows us to determine the sign of the intensity changes. Indeed, since we know that the intensity of amide II in decreasing with time, any positive correlation with amide II indicates a decreasing intensity. Such frequencies are indicated by a downward arrow in the left column of Table 1. Conversely, any positive cross-peak with the amide II′ band indicates an intensity increasing with time.

Such frequencies are indicated by an upward arrow in the left column of Table 1.

In summary, from the 2D analysis of the exchange data we find that process can, in a first approximation, be modeled by three components: a slow component which can be assigned to β-sheet, shifting from 1633 to 1622 cm^{-1}; a faster β-sheet component shifting from 1640 to an unidentified frequency, though likely to be superimposed to the 1633 cm^{-1} slow β-sheet; and "turn" structures.

To gain more information into the fast β-sheet component, we attempted to "reconstruct" its infrared spectrum by subtracting a late difference spectrum (60−30 min) supposed to contain essentially slowly exchanging β-sheet contribution from an early one (2−1 min) which contains both the slow β-sheet and fast β-sheet components. The same procedure was applied to the (120−60 min) and (4−2 min) spectra and the results were averaged. Subtraction was scaled in such a way that the contribution from the slow β-sheet component was minimal near 1622 cm^{-1}. The reconstructed component is shown in the upper right corner of Figure 5. Interestingly, the frequency of the maximum in the amide II′ (1465 cm^{-1}) is identical to that found from the 2D correlation analysis for the fast component. Whether the 1465 cm^{-1} amide II′ component belongs to the second type of β-sheet and/or to turn components cannot be decided here.

Streptavidin−Biotin. Figures 3 and 4 indicated that deuteration is slower for streptavidin when it binds its ligand biotin. In the left panel of Figure 5 the difference spectra for the streptavidin−biotin complex are shown. As can be seen, the presence of the ligand does not greatly modify the kinetics of deuteration of streptavidin and the characteristic features of the difference spectra. The 2-D anticorrelation map for the streptavidin−biotin complex is also nearly identical to that of streptavidin alone, confirming that the spectral components are the same (not shown). One of the main visible difference that appears in Figure 5 is that the S-shaped band with a minimum at 1678 cm^{-1} and a maximum at 1663 cm^{-1} disappears more slowly for the streptavidin−biotin complex. In fact it can still be observed in the 600−360 min difference spectrum. To illustrate this further we have subtracted the 60−30 min difference spectrum for the protein alone from the corresponding difference spectra for the biotin−protein complex. The result of the subtraction is the effect of biotin binding on the difference spectra. It is shown in the upper left panel of Figure 5. As can be seen the spectrum for the biotin-induced component and that for the fast exchanging structures computed previously (Figure 5, right panel) are almost similar but obviously different from the slow β-sheet difference spectrum. Furthermore, the biotin-induced difference spectrum presents a maximum near 1640 cm^{-1}, a frequency previously assigned to the fast exchanging β-sheet contribution. From this, we conclude that biotin binding retards the exchange of the fast exchanging β-sheet component while the exchange of the slow β-sheet is affected to a lesser extent. We therefore conclude that the presence of the ligand prevents exchange of parts of the β-barrel in the protein.

Discussion

Structure of Streptavidin. The protein has a closed β-barrel with eight antiparallel strands as its central core. Approximately half of the amino acid residues are part of this β-barrel, the other half consists mainly of loops connecting the β-strands. In Table 2 the distribution of the amino acid residues over various secondary structure classes is listed. In the available X-ray structures, not all residues are included (N- and C-terminal parts are missing), and therefore, the numbers in Table 2 should be interpreted with caution.

Interestingly, from the crystal structure, we know that the β-strands in the barrel vary in length, from 5 to 13. Four monomers containing each one β-barrel form a tetramer, and in this superstructure, the longer strands of the barrels are involved in the intersubunit contacts and thus buried, while the shorter ones are exposed to the solvent. The difference in solvent exposure and the fact that the parts of β-sheet with longer strands are believed to be more stable make it plausible that the amide proton exchange of the longer strands occurs more slowly. Kleffel et al.[28] have previously found a correlation between the average length of β-strands and the frequency of β-sheet absorption band near 1630 cm^{-1}. The longer the strands, the lower the frequency. According to the results presented here, biotin would not affect the exchange of the longer strands forming the core of the tetramer.

Structural Differences of the Apo And Holo Proteins. X-ray crystallographic studies have shown that the structure for the free and biotin-associated forms of streptavidin are very similar. However, in regions involved in the binding of the ligand, structural differences have been observed. There is experimental evidence that the conformational and dynamical properties of the loop between the β-strands 3 and 4 (comprising residues 45−52) are modified by the presence of the ligand. Studies by Freitag et al.[10] on streptavidin have shown that in the absence of the ligand the loop may adopt various conformations depending on the protein−protein interactions in the particular crystal type. Generally, the loop adopts an open conformation, with residues 50−52 in a 3_{10} helical structure. In certain crystals, the loop is disordered and cannot be traced in the electron density map; in others, the loop adopts the "closed" conformation also found in the presence of the ligand. The temperature B-factors for the atoms in the loop when no ligand is present are comparable to the average B-factor for the main chain atoms in the protein. In the absence of the ligand, the B-factors for the loop atoms are considerably higher, suggesting that in the absence of biotin the loop residues are mobile. In their X-ray studies on apoavidin, Livnah et al.[29] found the 3−4 loop to be disordered while Pugliese et al.[30] found the closed conformation. They noted however that the B-factors for the loop atoms were higher in the absence of the ligand than in its presence. Proteolysis experiments on the avidin−biotin system[31] have shown that, in the absence of ligand, the binding loop is susceptible to cleavage, which is not the case when biotin is bound. This shows that, in solution, the 3−4 loop adopts a different conformation in the absence of ligand, one that is perhaps in more mobile and flexible than in the holoprotein.

The small differences in the IR spectra observed for the free and biotin-bound forms of the protein are entirely consistent with the limited small changes in the crystal structure upon binding of the ligand. The structural differences observed in the studies cited above for the 3−4 loop may explain some of the differences in the H/D exchange rates observed by IR spectroscopy. The small difference in protein conformation as detected by IR spectroscopy might be induced by this limited conformation change.

Study of the thermally induced denaturation of streptavidin has shown an increased stability of the protein in the presence of ligand. Indeed remarkable is the change in the midpoint temperature for thermal denaturation T_m, upon binding of the ligand. For streptavidin T_m increases from 75 to 112 °C.[32] The increased stability has been interpreted in terms of an enhanced cooperativity of the thermal unfolding of the four subunits in holoprotein, due to stronger intersubunit association.[32] From the crystal structures we know that the biotin-binding site inside the barrel is made up by tryptophan indole groups. One of these groups is donated by the neighboring monomer. If biotin binding results in increased rigidity of the tryptophan rings one has a likely mechanism to explain the enhanced stability of the tetramer upon ligand binding.

Recent X-ray studies on streptavidin[10] revealed no systematic change in the quaternary structure of the tetrameric protein that can be associated with biotin binding, indicating that only the stability of the tetrameric form is modified upon ligand binding. The increased stability of the protein may be related to the protection of a number of amide groups against exchange. As mentioned above, the inter-subunit contacts in the tetramer are mainly between the strands of four β-barrels. It is therefore plausible that an increased rigidity of the tetrameric form results in inhibition of exchange of some β-strands.

In conclusion, the combination of the IR spectroscopy technique with 2D FTIR spectroscopy with H/D exchange as external perturbation was able to resolve the IR spectra into much greater details than static IR spectroscopy. Furthermore, changes in the protein dynamics as measured by amide H/D exchange kinetics could be compared in the presence and in the absence of ligand. Which secondary structure type was most affected by biotin binding on streptavidin was determined.

(28) Kleffel, B.; Garavido, R. M.; Baumeister, W.; Rosenbusch *EMBO J.* **1985**, *4*, 1589.

(29) Livnah, O.; Bayer, E. A.; Wilchek; M.; Sussman, J. L. *Proc. Natl. Acad. Sci. U.S.A.* **1993**, *90*, 5076.

(30) Pugliese, L.; Malcovati, M.; Coda, A.; Bolognesi, M. *J. Mol. Biol.* **1994**, *235*, 42.

(31) Ellison, D.; Hinton, J.; Hubbard, S. J.; Beynon, R. J. *Prot. Sci.* **1995**, *4*, 1337−1345.

(32) González, M.; Bagatolli, L. A.; Echabe, I.; Arrondo, J. L. R.; Argaraña, C. E.; Cantor; C. R.; Fidelio; G. D. *J. Biol. Chem.* **1997**, *272*, 11288.